virtual

Open access
virtual testing protocols
for enhanced
road user safety

Scientific publication on child model applications in VIRTUAL

WP number: 2
Deliverable: D2.3

This project has received funding from the European Union's Horizon 2020 research and innovation programme under grant agreement No 768960.

Scientific publication on child model applications in VIRTUAL

Work package 2, Deliverable D2.3

Please refer to this report as follows:
Svensson, M., Iraeus, J., Meredith, L. Wågström, L. (2021). Scientific publication on child model applications in VIRTUAL, Deliverable D2.3 of the H2020 project VIRTUAL.

Project details:	
Project start date: Duration: Project name:	01/06/2018 48 months Open access virtual testing protocols for enhanced road user safety – VIRTUAL
Coordinator:	Astrid Linder, Adj Prof, PhD – Research Director Traffic Safety Swedish National Road and Transport Research Institute (VTI) Regnbågsgatan 1, 417 55 Lindholmen, Göteborg, Sweden
	This project has received funding from the European Union's Horizon 2020 research and innovation programme under grant agreement No 768960.

Deliverable details:	
Version: Dissemination level: Due date: Submission date: Online location:	Final PU (Public) 31/01/2021 (original date: 30/09/2020) 31/01/2021 https://secure.webforum.com/atvirtual/doc/?dfRefID=791

Lead contractor for this deliverable:
Mats Svensson – Chalmers

Report Author(s):	Svensson, M., Iraeus, J., Meredith, L. (Chalmers), Sweden Wågström, L. (Volvo), Sweden

Revision history

Date	Version	Reviewer	Description
27/01/2021	Preliminary draft 1	Krašna, S. (UL), Slovenia	Review round 1 - Rating
30/01/2021	Final draft #	Names of Task leader: Mats Svensson (Chalmers) WP leader: Mats Svensson (Chalmers) QM, Coordinator	
31/01/2021	Final report	Name of English language reviewer: NA	
31/01/2021	Final deliverable	Astrid Linder – VTI ➔ EC	

Table of contents

Executive summary

As road users come in different sizes, ages, and genders WP2 will create the human body model (HBM) resources used in the VIRTUAL project activities in WP3,4 and 5. Specifically, WP2 will provide a set of HBMs ready for implementation in specified demonstration cases for seated occupants, Vulnerable Road Users (VRUs) and erect passengers in public transport. WP2 will exploit existing HBMs and supporting software previously developed in the national (VIVA) and EU Funded (PIPER) projects. These open-source resources will be further enhanced to extend their application and availability to the community.

One main goal of the VIRTUAL project is to define the general workflow of a virtual test procedure that starts with a physical test that works as a reference for validation of the virtual simulation. The virtual simulation set-up is then compared to the physical test set-up by replicating the physical test conditions, to verify the validity of the virtual simulation test set-up. The virtual simulation test set-up will then be employed to study a range of parameter variations. These variations can be in the crash configuration, such as crash pulse shape, delta-v, collision angle etc. The variations can also be in the occupant posture, seat adjustment, occupant size and gender etc. This range of variations will enable a far more robust assessment taking the real-world variability into account. There will however not be a dedicated physical loading device for the child seat virtual test chain in VIRTUAL. Instead, a Q6 dummy and an LS-Dyna Q6 dummy-model is used to verify the virtual simulation test set-up.

The current document reports the results of **Task 2.3: "Child HBM development for Child Safety Applications".** The child model developed in the European FP7 project PIPER provides new opportunities to assess child safety and is the topic of Task 3.4. In WP2 the PIPER model has been reviewed and now supplemented with the desired IDS (Injury Detction Systems) to make it possible to export relevant injury risks. In WP3 it was decided to focus the child protection use cases on the 6-year-old category in frontal impact conditions. Milestone M3.5 identified the following suitable existing IDS:

- HIC_{15} (where there is hard contact).
- Cumulative 3ms resultant Head Acceleration.
- Upper Neck Tension Force Fz.
- Upper Neck Moment My.
- Thorax Acceleration Cumulative 3 ms.
- Thorax Chest Deflection Dx.
- Lower Lumbar Load Cell Force.
- Lap belt force (booster seats only).
- Horizontal and Vertical Head Excursion.

Milestone M3.5 identified the criteria of Table 1 displaying the Q6 dummy injury criteria and AIS3+ injury risk limits from the UN Regulation 129.

Table 1: Q-Series injury criteria and limits from UN Regulation 129, EEVC Working Groups 12 and 18, the CASPER and EPOCh projects – Q3 to Q10 (Visvikis et al., 2014)

Source	Risk of injury	Head HIC (15/36)	Head A 3 ms (g)	Neck +Fz (N)	Neck +My (Nm)	Chest Dx (mm)	Chest A 3 ms (g)	Abdom. P (bar)
Q6 dummy								
UN R129 limits		**800**	**80**	*	*	-	**55**	-
EEVC	UN R94 (scaled)	986	82	1,824	94	42	-	-
	AIS≥3 20% CM	1,097	92	2,101	118	35	-	-
	AIS≥3 20% LR	1,083	89	2,101	118	33	-	-
	AIS≥3 50% CM	1,306	101	2,304	143	44	-	-
	AIS≥3 50% LR	1,389	109	2,304	143	49	-	-
CASPER	AIS≥3 50% SA	-	-	-	-	-	-	1.09

Validation data for the seating environments in VIRTUAL representing loading from a child occupant was generated in milestone M3.4, where a Q6 child dummy was placed on a Dorel "RodFix" booster seat suitable for children in the ages 3,5 up to 12 years, conforming to the ECE R44/04 norm. The Q6 dummy and the booster seat were then placed on the ECE R129 seat bench and run under the ECE R129 frontal collision test specifications.

In the current study a new ECE R129 test set-up was implemented in LS-Dyna and this will be an open-source model, published on the VIRTUAL Open VT platform. This model included the seat geometry and seat cushion stiffness properties as well. The current study reproduced the physical Q6 child dummy tests using an LS-Dyna Q6 child dummy model. A simulation matrix was run with paired comparisons between the Q6 and the PIPER 6yo models.

The core result of this deliverable (D2.3) is the scientific paper manuscript attached to this short main report. The focus of this paper was to develop a method for adapting the Q-series risk curves to be used with the PIPER HBM. This was intended to be a method that could be developed and implemented without rerunning the original accident reconstructions. The 3ms resultant head acceleration of the PIPER model was related to the Q6 response using linear regression, and this relationship was applied to a previously defined Q-series head injury risk curve, adapting this to the PIPER model.

1 Paper manuscript

A METHOD TO ADAPT Q- SERIES CHILD ATD INJURY RISK CURVES TO THE PIPER HUMAN BODY MODEL

Johan Iraeus[1], Pooja Umeshkumar[2], Dag Thuvesen[2], Lauren Meredith[1], Mats Svensson[1]

[1] Division of Vehicle Safety, Department of Mechanics and Maritime Sciences, Chalmers University of Technology, Sweden

[2] China Euro Vehicle Technology, Sweden

Keywords: Child Safety, Human Body Model, PIPER, Q6 Dummy, Injury Risk

A METHOD TO ADAPT Q- SERIES CHILD ATD INJURY RISK CURVES TO THE PIPER HUMAN BODY MODEL

Johan Iraeus[1], Pooja Umeshkumar[2], Dag Thuvesen[2], Lauren Meredith[1], Mats Svensson[1]

[1] Division of Vehicle Safety, Department of Mechanics and Maritime Sciences, Chalmers University of Technology, Sweden

[2] China Euro Vehicle Technology, Sweden

Keywords: Child Safety, Human Body Model, PIPER, Q6 Dummy, Injury Risk

2 ABSTRACT

Child safety crash testing is expected to become complemented with virtual testing. The PIPER Human Body Model (HBM) is a recent open-source child occupant model. Currently the PIPER HBM lacks injury risk functions that can interpret injury criteria outputs into risk. The aim of the current study was to develop a method for adapting the Q-series risk curves to be used for PIPER HBM, without rerunning the original accident reconstructions.

A finite element (FE) model representing an ECE R129 sled test set up was implemented in LS-Dyna. A FE high-back booster child seat model was validated using a validated model of the Q6 child anthropometric test device (ATD). A matrix of frontal impact simulations was run in matched pair simulations of the PIPER 6YO and the Q6 model.

The 3ms resultant head acceleration of the PIPER model was related to the Q6 response using linear regression, and this relationship was applied to a previously defined Q-series head injury risk curve, adapting this to the PIPER model.

The current results are likely only applicable for non head contact cases in frontal collision in a high-back-booster seat.

3 INTRODUCTION

While the number of child fatalities and injuries in motor vehicle crashes has decreased over the years as a result of improved safety systems and increased child restraint usage, there is still a need for further improvements (Bohman, 2013). Globally, road traffic injuries are currently the leading cause of death for children and young adults aged 5–29 years (World Health Organization, 2018). Improvements in vehicle safety systems can be driven through improved regulatory assessment of such systems. Currently, assessment of the efficacy of child safety systems is conducted using physical crash tests with anthropometric test devices (ATDs), also called crash test dummies, equipped with a variety of measuring devices to determine the response of the dummy under different loading conditions. These responses can then be correlated to injury by using pre-established injury criteria and risk functions.

The most recent child ATDs are the Q-series family (Humanetics Q series, 2020). The Q-series ATDs are sized to represent different aged children. The Q6 ATD is one of the Q-series ATDs and represents the anthropometry and biofidelity of a 6-year-old child (Wismans et al., 2008). For injury assessment, it is equipped with a 3-axis accelerometer in head, thorax and pelvis, as well as a 6-axis load cell in the upper neck, lower neck and lumbar spine, a 3-axis angular rate sensor in the head and a displacement sensor in the chest. A set of injury risk curves were developed corresponding to the Q6 dummy and were used to set threshold levels for injury based on these measured responses (Visvikis, Pitcher, Carroll, Cuerden, & Barrow, 2013; Wismans et al., 2008).

Specifically, risk curves have been developed for Regulation to assess injury responses for the full range of Q-series ATDs in various restraint systems during frontal and oblique collisions (UN regulation R129, 2013). This regulation requires assessment of both head and chest acceleration as well as the head injury criterion (HIC). The thresholds for injury used to assess the injury response for tests conducted in accordance with this regulation were largely set from the work by Wismans et al. (Wismans et al., 2008), which used accident reconstructions to develop injury risk curves for the head, thorax and neck of a 3 year old child in frontal collisions. However, due to limited data, neck risk curves were not achievable. To overcome this limitation, a second set of injury risk curves were developed by scaling down from adult risk curves, allowing for neck injury risk curves (Palisson, Trosseille, & Lesire, 2007). More recent investigations supplemented the original set of accident reconstructions, providing a larger dataset to allow for neck and abdominal injury risk curve development (Beillas et al., 2012; Johannsen, Trosseille, Lesire, & Beillas, 2012). These were not, however, adopted in Regulation R129.

Due to practical difficulties, current testing of vehicle safety systems using physical crash tests and ATDs is unable to assess the full range of accident situations which occur in the real world. Virtual testing, using large parameter studies, has the potential to provide a more robust safety assessment (Iraeus & Lindquist, 2016; Perez-Rapela, Forman, Huddleston, & Crandall, 2020). As well as being able to assess a wider range of crash configurations that can accommodate the wide variation of crashes in real world accidents, virtual testing can also provide a platform to easily assess injury outcome based on crash severity, occupant size and seated posture of the vehicle occupant. Finite element (FE) human body models (HBMs) allow for a detailed representation of different body parts, both in terms of geometry and material properties. Thus, these FE HBMs have the potential to predict injury directly at the tissue level, providing a less restricted and potentially improved prediction of injury outcome than can be achieved from physical testing with ATDs. Specifically, the spine of HBMs is more biofidelic and much more flexible compared to ATDs, in particular for axial rotation. Based on work on adult FE HBMs, it is expected that the child FE HBMs can reach a higher degree of biofidelity compared to virtual ATDs (Lanner et al., 2010).

The PIPER child FE HBM is one such model representing children of ages between 1.5 and 6 years (Beillas et al., 2016). The PIPER FE HBM has been used previously to examine child injury tolerances and body responses to traumatic impact (Giordano, Li, & Kleiven, 2017; Pezzutti, 2017). However, due to a paucity of information surrounding child injury tolerance levels based on post-mortem human subjects, these studies largely relied on injury criteria which had been developed based on adult injury risk curves. Only one investigation by Mertz et al. presented injury risk curves for children (Mertz, Prasad, & Irwin, 1997). However, the injury risk curves developed in this work aimed to provide injury assessment of ATD responses rather than that of a virtual HBM.

It is apparent that ATDs exhibit different kinetics and kinematics, and thus different injury responses to FE HBMs under the same loading conditions (Mizuno, Iwata, Namikiri, &

Tanaka, 2009; Sarfare, Maheshwari, Duong, & Belwadi, 2018; Zhang et al., 2007). Additionally, markedly differing acceleration responses for the chest and pelvis for different booster conditions has been found, indicating that differences in restraint systems may also affect the injury responses (Sarfare et al., 2018). Therefore, it is essential that the injury risk curves are designed and validated specifically for the appropriate HBM. In a recent study, an attempt was made to create linear regression models, relating the injury response of the PIPER FE HBM to the Q6 ATD under similar load conditions (Holtz J, 2019). Using this approach, the predefined Q6 risk curves can be used together with the PIPER model. However, no child restraint systems, e.g. booster cushion or booster seat with backrest were included in this study. As it is a requirement under European law for children under 150cm, or up to 12 years of age, to be travelling in a child restraint approved to Regulation R129 (European Commision, 1991), there is a need to expand on previous studies to validate injury risk curves under these conditions.

As of today, a consistent set of child HBM injury risk curves corresponding to ATD risk curves are not available. The aim of this work was to develop a method that can be used to adapt the Q-series risk curves to be used for PIPER HBM, without rerunning the original accident reconstructions. This will be exemplified on the 3ms resultant head acceleration risk curve for a 6-year-old child.

4 METHOD

The method to adapt Q-series risk curves to the PIPER HBM can shortly be summarized as follows; a Q-series ATD and a similar sized PIPER HBM is positioned in a validated vehicle seat model, including a child restraint model. A set of matched paired simulations (Q-dummy and PIPER) are run, representing different crash configurations, with different crash severities. Relate the PIPER output sensor signals to the Q-dummy signals, by using for instance linear regression. Finally, for each risk curve, first scale it to the age of interest, then apply the previously defined relationship to rescale the risk by parameter substitution, to form a risk curve adapted to the PIPER model.

For the present study, the method will be exemplified using a validated FE model of a high back booster child seat positioned in a R44 environment (UN regulation R44, 2008). The metal structures of the R44 sled were modelled as rigid. The material data for the R44 seat cushion was calibrated according to R44 (Annex17). A 2.75-kilo hemispherical impactor was dropped on the foam and the acceleration experienced by the impactor during the impact was recorded. The material's stress-strain curve was modified to match the acceleration-time from a physical impactor test (Hynd, Pichter, Hynd, Robinson, & Carroll, 2010). A FE model of the Maxi-Cosi Rodifix booster seat was positioned on the seat cushion, and attached to the ISOFIX mounting points, to complete the setup.

The FE model of the R44 environment and child seat was validated to a physical test including a Q6 ATD. In a pre-simulation, a validated Humanetics Q6 version 2.1 FE model (Humanetics, 2017) was positioned to match the position of the Q6 ATD in the physical test. Constant force (300 N) cables attached to rigid parts of each segment of the dummy, pulled these to the corresponding coordinates of the physical ATD. Then, the FE model nodes were replaced by the updated nodal coordinates from the pre-simulation, effectively zeroing out the stresses and strains from the pre-simulation.

A standard 48mm wide (without pre-tensioner or load limiter) high stretch (12-14%) FE 3-point seatbelt was routed over the lap and the chest similar to the physical test. During the first 50ms of the simulation, the lap portion and the diagonal portion of the belt was tensioned with 50N (as described in R44), and then the pulse from the physical test was applied to the rigid sled structure. The FE model of the child seat and R44 environment was validated by comparing the child seat kinematics and dummy responses to the physical test results. The positioned Q6 FE model is compared to the physical test setup in Figure 1 (left and mid subfigures).

Figure 1. The physical test setup (left), the FE model including the FE Q6 ATD model (mid), and the FE model including the 6year old PIPER FE HBM (right).

A second FE model was created by replacing the Q6 FE model with the 6 year old PIPER FE HBM v 1.0.0 (Beillas et al., 2016). The PIPER model was positioned to match the Q6 ATD as close as possible, by first matching the H-point, and then apply constant force cables (300N) to pull PIPER body parts (T1, hands, feet, femur, humerus and forearm) as close as possible to that of the Q6 ATD. Similar to the Q6 FE model, the original nodal coordinates were replaced by the results from the pre-simulation, to zero out stresses and strains. Finally, the belt was re-routed to match the routing over the Q6 ATD chest and lap. The model can be seen in *Figure 1* (right subfigure).

Next step was to run matched pair simulations of different crash severities (covering risks from zero to one), using both FE models. The crash pulse was modelled according to (Iraeus

& Lindquist, 2016). Here, real life crash pulses were parameterized using change in velocity (DV), pulse duration, pulse angle, and pulse shape (parametrized using eigenvectors). In this study DV was varied between 30 km/h and 80 km/h in steps of 10 km/h and pulse duration in two levels, 94 ms and 110 ms. A constant crash angle of zero degrees and the average pulse shape from the Iraeus and Lindquist study was used.

To exemplify the method, the head 3ms acceleration was extracted from each pair of simulations. For both models, each linear acceleration component (x, y, and z) was filtered according to recommendations (SAE J211, 1995), before the result acceleration was computed and the 3ms clip was calculated. Next, using the results from all paired simulations, the head 3ms clip from the PIPER model was expressed as function of the head 3ms clip from the Q6 ATD, using linear regression (LM function) in R v 4.0.2 (R Core Team, 2020).

Finally, the Q3 ATD 3ms head acceleration AIS3+ risk curve from (Johannsen et al., 2012) was rescaled to Q6 by multiplying the with scaling factor 1.1, scaling according to (Mertz & Prasad, 2000), as defined in (Johannsen et al., 2012). The PIPER 6-year-old adapted risk curve was then produced by performing a parameter substitution in the original 3ms head acceleration AIS3+ risk curve.

The Q6 model was run with LS-DYNA (LSTC, Livermore, Switzerland), Version: mpp s R11.1.0 Revision: 139588, and the PIPER HBM was run with LS-DYNA, Version: mpp s R9.3.1 Revision: 140922. Model pre-processing was done in ANSA version 20.1.3 (BETA CAE Systems, Switzerland) and post processing in META version 20.1.3 (BETA CAE Systems, Switzerland).

5 RESULTS

The results from the calibration of the R44 seat foam can be found in Appendix A. The peak acceleration as well as loading and unloading stiffness were matched well.
The FE model of the R44 sled and child seat showed a close match to the physical test. In *Figure 2* the time history of the result head acceleration is compared. In Appendix B more signals are compared.

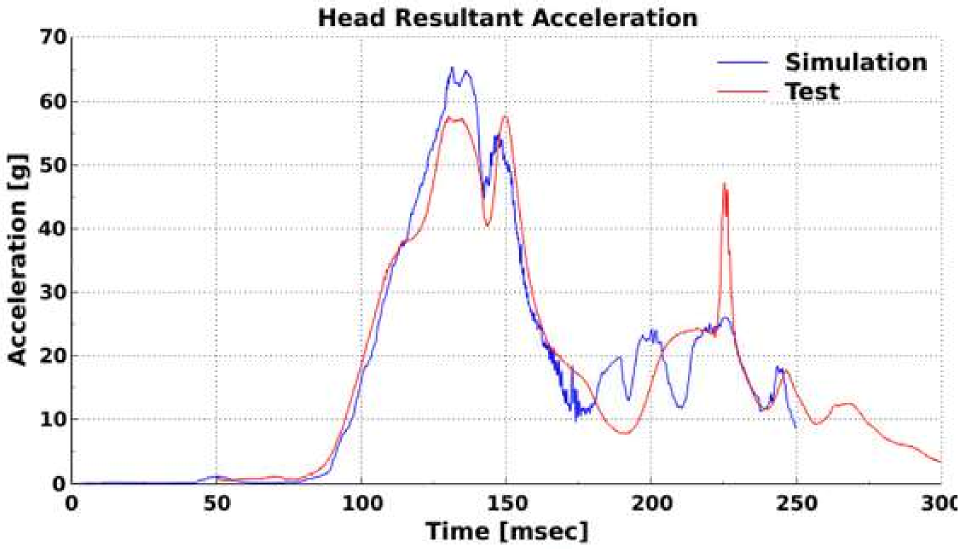

Figure 2. Comparison of resultant head acceleration, between physical test (red) and FE simulation (blue)

The linear regression model, PIPER 3ms head acceleration as dependent variable and the Q6 3ms head acceleration as independent variable was significant (F-test, $p<0.001$), and the intercept needed to be included, not to violate the model assumption of normally distributed residuals with a zero mean value. The regression model together with the individual simulation results is plotted in *Figure 3*. The results of the simulations are also found in Appendix C. For all matched pair simulations, the Q6 FE model predicted higher 3ms head accelerations compared to the 6-year-old PIPER FE model.

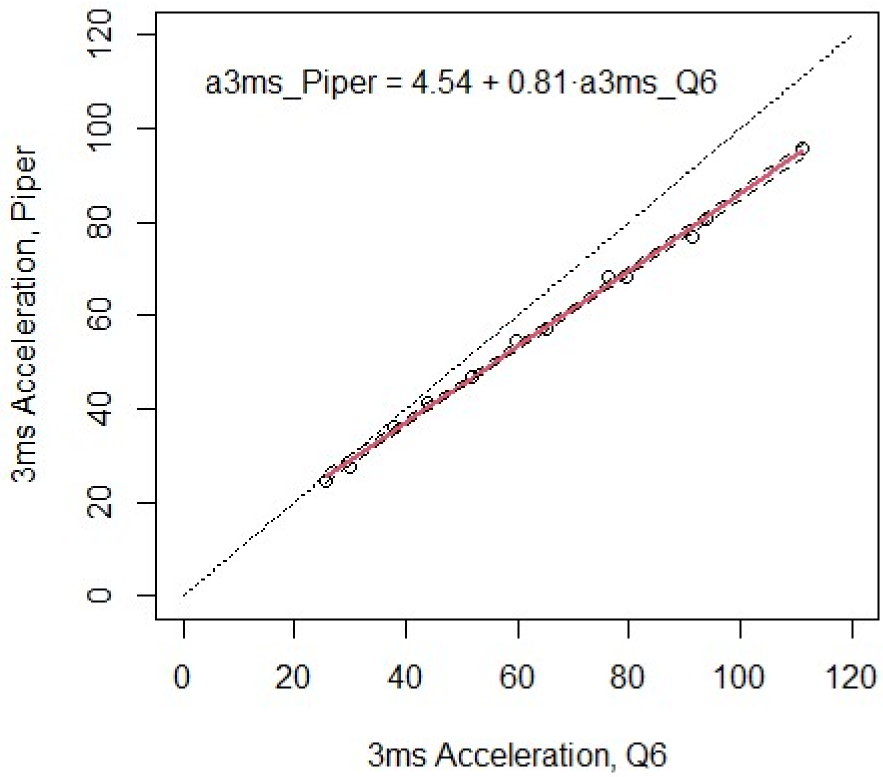

Figure 3. Results of the matched pair simulations (dots), and linear regression model (red line) relating the 3ms head acceleration in PIPER to the 3ms head acceleration in Q6. The dashed line represents the 95th percentile confidence bands and the dotted line is the 45-degree line.

The 3ms head acceleration risk curve in (Johannsen et al., 2012) is based on survival analysis using the parametric Weibull distribution, and can be described using cumulative distribution function (CDF) in Equation 1,

$$F(a_{3ms,Q3}) = 1 - e^{-\left(a_{3ms,Q3}/\lambda\right)^{k}} \qquad \text{(Eq. 1)}$$

with λ being the scale factor and k being the shape factor of the distribution. The risk curve was originally derived for the Q3 ATD. By scaling the acceleration to Q6 using the scaling factor (1.1) from (Johannsen et al., 2012), and then introducing the relationship established by the linear regression (*Figure 3*), according to Equation 2, and finally do a parameter substitution relating the 3ms acceleration in the FE Q3 ATD to the 6 year old FE PIPER HBM, using equation 3.

$$a_{3ms,Piper\ 6yr} = 4.54 + 0.81 \cdot 1.1 \cdot a_{3m\ ,Q3} \qquad \text{(Eq. 2)}$$

$$F\left(a_{3ms,Piper\ 6yr}\right) = 1 - e^{-\left(\frac{a_{3ms,Piper\ 6yr}-4.54}{0.81\cdot 1.1}\Big/\lambda\right)^{k}} \quad \text{(Eq. 3)}$$

Using Equation 3 the adapted risk curve can be plotted and compared to the original Q3 risk curve, see *Figure 4*. Other risk curves, e.g. survival analysis based on log-normal or log-logistic distributions or logistic regression will have other CDFs, but the same principles can be applied.

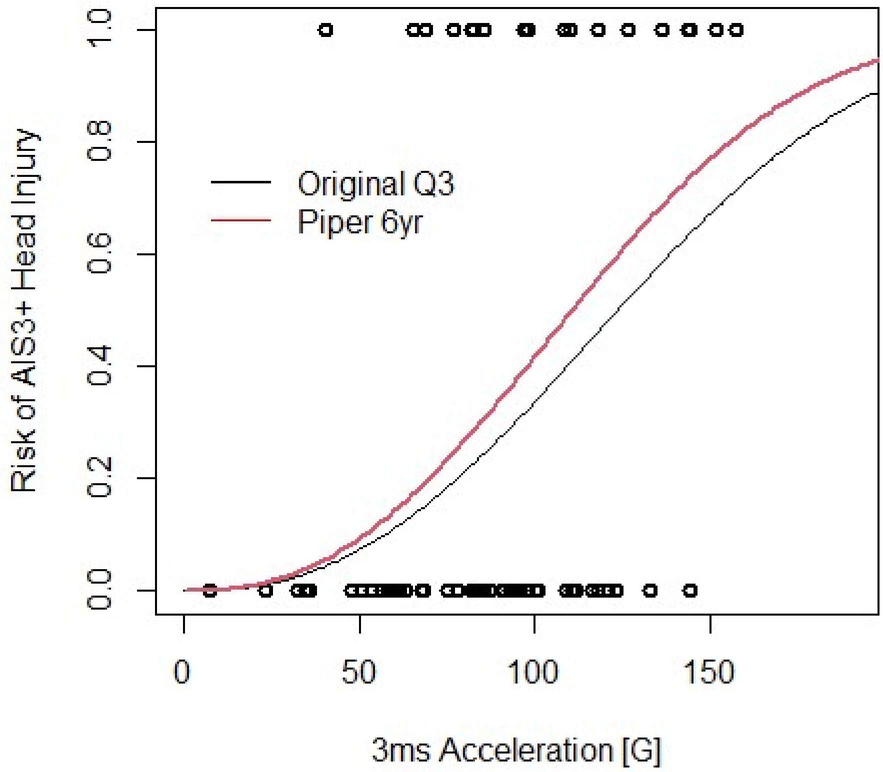

Figure 4. The adapted 3ms head acceleration risk curve for the PIPER 6-year-old FE HBM (red), compared to the original Q3 risk curve (black). The original unscaled results from the reconstructions shown as dots.

6 DISCUSSION

The present study has similarities with (Holtz J, 2019), the major difference being that that in the current study the 6 year old PIPER FE HBM was placed on a high-back-booster seat whereas Holtz placed it directly on the R129 seat bench, and used a different acceleration pulse. Interestingly the two studies arrive at different results. In the current study the predicted peak head acceleration of the PIPER model was about 20% lower than the peak head acceleration of the Q6 ATD model. In the Holtz study it was the other way around, the PIPER model predicted about 40% higher head acceleration compared to the Q6 ATD model. This indicates that the results are sensitive to the boundary conditions, which was also concluded in a study of (Sarfare et al., 2018) where the authors compared three different configurations, low back booster CRS, high back booster CRS and no child seat (comparable to the Holtz et al. study). Although only analyzing one load condition, Sarfare also found that the 6 year old PIPER model predicted lower peak head accelerations compared to the Q6 ATD model for the high back booster and no CRS, although much closer for the for the high back booster CRS. For the low back booster CRS, the 6 year old PIPER HBM predicted higher peak head acceleration than the Q6 ATD model.

In the current study it was observed that the more flexible spine in the PIPER HBM led to more upper body axial rotation compared to the Q6 ATD model, see *Figure 5*. This also means that the inferior part of the cervical spine moves further forward in the PIPER model, leading to a longer ride down distance for the head. It is hypothesized that this mechanism leads to the lower head peak acceleration in the PIPER HBM compared to the Q6 ATD model. This indicates that differences seen in the three compared studies, might be related to the seat belt interaction, and in particular the interaction with the shoulder belt. The seat belt anchorage points defined for the ECE R129 environment, used in the current study as well as in the Holtz study, most likely do not correspond well to modern vehicle rear seat geometries. In contrast the Sarfare environment was based on a far more recent 2012 Toyota Camry. Future studies should investigate the sensitivity of belt geometry, and in particular of the D-ring position.

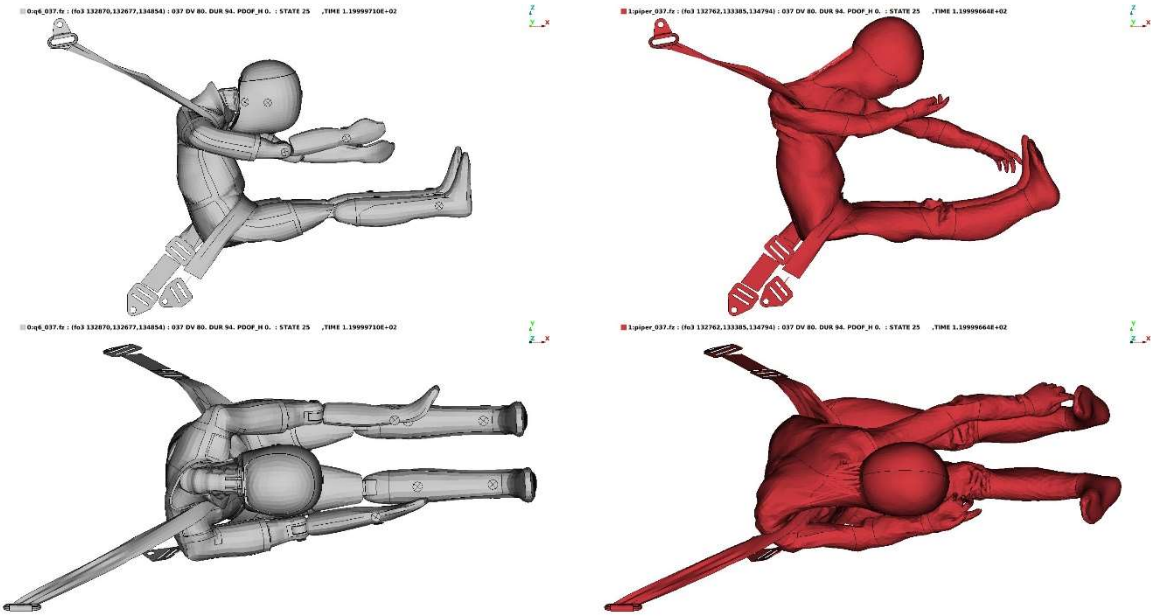

Figure 5. Comparison of the Q6 ATD model kinematic at time 120ms (close to peak head acceleration) (grey), to the 6-year-old PIPER HBM kinematic at time 120ms (red)

In the presented method the Q3 ATD risk curve was adapted to the 6 year old PIPER HBM using parameter substitution in the CDF. It should be noted that this is equivalent to scaling the risk curve abscissa (x-axis). Thus, in cases where the underlying CDF is not known, an adapted risk curve can be constructed by first digitalized the curve, and then rescale the x-values to the appropriate occupant size, followed by rescaling a second time using the linear relationship according to Equation 2.

Although the current study presents a method to adapt Q-series ATD risk curves to the PIPER model, it should be noted that there are a lot of uncertainties about the risk curves developed for the Q-series ATDs. In the EEVC work (Wismans et al., 2008) many risk curves were developed using accident reconstructions, both using logistic regression and survival analysis. Risk curves were presented for HIC36, the head 3ms clip, and the chest deflection, at AIS2+ to AIS 4+ severity levels. However, when this data was later reanalyzed together with additional data, also considering the width of the confidence intervals, only one risk curve based on the head 3ms acceleration could be constructed. Obviously, if there are doubts about the underlying risk curves, there is a risk that additional scaling of the results, as proposed in the current study, will deteriorate the quality of the risk curves even more.

This study is based on the assumption that the head does not contact any hard surface. This is a reasonable assumption when comparing the 70 original reconstructions (Johannsen et al., 2012), of which only 20-25% included a contact. Additionally, about 20-25% included self-contact, mainly between the chin and chest (which also occurs in the simulations in the current study). The 3 ms head resultant acceleration for predicting head injury risk has its origin in studies on head impact (Got, Patel, Fayon, Tarriere, & Walfisch, 1978), so when there is no direct head impact it must be interpreted with care.

Another limitation with the current study is that it is only valid for frontal impacts. Additionally, it has been indicated that it is only valid for high back booster seats with a vehicle layout similar to the ECE R129 geometry. However, as it is required under the European law for children under 150 cm, or up to 12 years of age, to travel in child restraints (European Commision, 2015), and typically high back booster seats are suitable up to an age of 8 years (Arbogast, Jermakian, Kallan, & Durbin, 2009), it is likely that the results of this study are appropriate for the 6 year old PIPER HBM under those conditions.

All the FE models used in this study, except the Q6 ATD model, are available as open source models.

7 CONCLUSION

The current study compared the responses and injury criteria outputs of the Humanetics Q6 v 2.1 FE model and the PIPER FE HBM v 1.0.0. The two child occupant models were placed in an FE model of a high back booster child seat positioned in an R44 environment. Frontal impact simulations were run at 12 different crash pulse conditions. A method was developed to adapt the Q-series risk curves to be used with PIPER HBM. The method was exemplified on the 3ms resultant head acceleration risk curve for a 6-year-old child. An important limitation is that the adapted PIPER HBM risk curves are valid only under the load conditions under which they were developed.

8 ACKNOWLEDGEMENTS

This study has received funding from the European Union Horizon 2020 Research and Innovation Programme under Grant Agreement No. 768960.

9 REFERENCES

Arbogast, K. B., Jermakian, J. S., Kallan, M. J., & Durbin, D. R. (2009). Effectiveness of belt positioning booster seats: an updated assessment. *Pediatrics, 124*(5), 1281-1286.

Beillas, P., Alonzo, F., Chevalier, M.-C., Lesire, P., Leopold, F., Trosseille, X., & Johannsen, H. (2012, October 29-31). *Abdominal twin pressure sensors for the assessment of abdominal injuries in q dummies: in-dummy evaluation and performance in accident reconstructions.* Paper presented at the 56th Stapp Car Crash Conference, Savannah, Georgia, USA.

Beillas, P., Giordano, C., Alvarez, V., Li, X., Ying, X., Chevalier, M.-C., . . . Kleiven, S. (2016). *Development and performance of the PIPER scalable child human body models.* Paper presented at the 14th International Conference on the Protection of Children in Cars.

Bohman, K. (2013). *Car Safety for Children Aged 4-12: real world evaluations of long-term injury outcome, head injury causation scenarios, misuse, and pre-crash maneuver kinematics.* (PhD thesis). Karolinska Universitet,

European Commision. (1991). *Council Directive 91/671/EEC of 16 December 1991 on the Approximation of the Laws of the Member States Relating to Compulsory Use of Safety Belts in Vehicles of Less than 3,5 Tonnes*.

European Commision. (2015). Mobility and Transport, Road Safety. Retrieved from http://ec.europa.eu/transport/road_safety/specialist/statistics/index_en.htm

Giordano, C., Li, X., & Kleiven, S. (2017). Performances of the PIPER scalable child human body model in accident reconstruction. *PloS one, 12*(11). doi:https://doi.org/10.1371/journal.pone.0187916

Got, C., Patel, A., Fayon, A., Tarriere, C., & Walfisch, G. (1978, 8-10 Novemeber). *Results of experimental head impacts on cadavers: the various data obtained and their relations to some measured physical parameters.* Paper presented at the 22nd Stapp Car Crash Conference, Denver, Colorado, US.

Holtz J. (2019, September 11-13). *Comparison of PIPER child human body model and Q6 Dummy analysing sensors of the HBM.* Paper presented at the International IRCOBI Conference, Florence (Italy).

Humanetics. (2017). *Q6 Child Dummy Model LS-DYNA, Release Version 2.1*. Retrieved from

Humanetics Q series. (2020). Retrieved from https://humanetics.humaneticsgroup.com/products/anthropomorphic-test-devices/child/q-series/q6-6-year-old-child

Hynd, M., Pichter, M., Hynd, D., Robinson, B., & Carroll, J. (2010). *Analysis for the development of legislation on child occupant protection*. Retrieved from https://circabc.europa.eu/sd/a/1900fc33-ce43-4265-8dd5-1564df985635/report-child-occupant-protection_en.pdf

Iraeus, J., & Lindquist, M. (2016). Development and validation of a generic finite element vehicle buck model for the analysis of driver rib fractures in real life nearside oblique frontal crashes. *Accident Analysis & Prevention, 95, Part A*, 42-56. doi:http://dx.doi.org/10.1016/j.aap.2016.06.020

Johannsen, H., Trosseille, X., Lesire, P., & Beillas, P. (2012, September 12-14). *Estimating Q-Dummy injury criteria using the CASPER project results and scaling adult reference values.* Paper presented at the Proceedings of IRCOBI Conference, Dublin, Ireland.

Lanner, D., Halldin, P., Iraeus, J., Holmqvist, K., Mroz, K., Pipkorn, B., . . . Kleiven, S. (2010). Evaluation of finite element human body models in lateral padded pendulum impacts to the shoulder. *International Journal of Crashworthiness, 15*(2), 125-142. Retrieved from http://www.scopus.com/inward/record.url?eid=2-s2.0-77954830202&partnerID=40&md5=618dfaf02a74162b5917c40d3ef56d1a

Mertz, H. J., & Prasad, P. (2000). *Improved neck injury risk curves for tension and extension moment measurements of crash dummies.* Paper presented at the Stapp car crash journal.

Mertz, H. J., Prasad, P., & Irwin, A. L. (1997). Injury risk curves for children and adults in frontal and rear collisions. *SAE transactions, 106*, 3563-3580.

Mizuno, K., Iwata, K., Namikiri, T., & Tanaka, N. (2009). Comparison of human FE model and crash dummy responses in various child restraint systems. *International Journal of Crashworthiness, 14*(2), 139-149.

Palisson, A., Trosseille, X., & Lesire, P. (2007, September 19-21). *Estimating Q3 dummy injury criteria for frontal impacts using the child project results and scaling reference values.* Paper presented at the International IRCOBI Conference, Maastricht, The Netherlands.

Perez-Rapela, D., Forman, J. L., Huddleston, S. H., & Crandall, J. R. (2020). Methodology for vehicle safety development and assessment accounting for occupant response variability to human and non-human factors. *Computer methods in biomechanics and biomedical engineering*, 1-16. doi:https://doi.org/10.1080/10255842.2020.1830380

Pezzutti, S. (2017). *Age–Related Perspectives on the Biomechanics of Traumatic Injury.* (Master Thesis). KTH, Retrieved from https://www.diva-portal.org/smash/get/diva2:1113430/FULLTEXT01.pdf

R Core Team. (2020). R: A language and environment for statistical computing. Vienna, Austria: R Foundation for Statistical Computing. Retrieved from http://www.R-project.org/

SAE J211. (1995). Recommended Practice: Instrumentation for Impact Test – Part 1, Electronic Instrumentation. In *SAE J211/1*: Society of Automotive Engineers.

Sarfare, S., Maheshwari, J., Duong, N., & Belwadi, A. (2018, Nov 12-14). *Comparative Responses of the PIPER 6YO Human Body Model and the Q6 ATD for Simulated Frontal and Lateral Impacts.* Paper presented at the 62nd Stapp Car Crash Conference, San Diego, US.

UN regulation R44. (2008). *R44: Uniform Provisions Concerning the approval of restraining devices for child occupants of power-driven vehicles ("child restraint system").* Geneva, Switzerland

UN regulation R129. (2013). *Regulation: 129 Uniform Provisions Concerning the Approval of Enhanced Child Restraint Systems Used on Board of Motor Vehicles (ECRS)*. Geneva, Switzerland

Visvikis, C., Pitcher, M., Carroll, J., Cuerden, R., & Barrow, A. (2013). *New UN regulation on child restraint systems-assessment of amendments to the new regulation, front and side impact procedures and Q-Series dummy family injury criteria* (Report number CPR 1801). Retrieved from https://op.europa.eu/s/oIEu

Wismans, J., Waagmeester, C., le Claire, M., Hynd, D., de Jager, K., Palisson, A., . . . Trosseille, X. (2008). *Q-dummies report: advanced child dummies and injury criteria for frontal impact* (TNO report 781710). Retrieved from http://resolver.tudelft.nl/uuid:d503e3a6-6b14-41f0-8219-5cadff813e79

World Health Organization. (2018). *WHO global status report on road safety 2018* (9789241565684). Retrieved from https://www.who.int/publications/i/item/9789241565684

Zhang, W., Kapoor, T., Tot, M., Altenhof, W., Howard, A., & Mizuno, K. (2007). *A comparison of the kinematics of a child finite element model and the hybrid III 3-year-old dummies in frontal crashes* (0148-7191). Retrieved from

10 Appendix A – Calibration of seat foam

The results of the seat foam calibration can be seen in Figure A- 1. As it is hard to establish a well-defined t_0, it was decided to align the curves at a force of 178N (a force level that was judged to be representative of the initial slope).

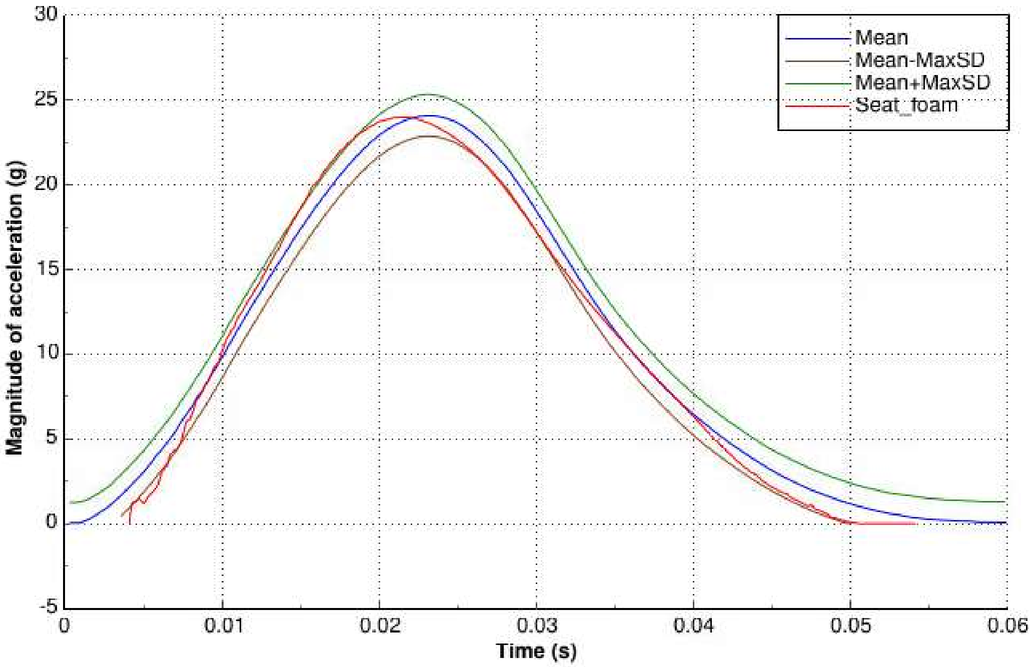

Figure A- 1. Calibration of foam properties for the R44 seat foam. "Seat-foam" denotes the simulation results.

11 Appendix B – Validation of R44 sled and child seat

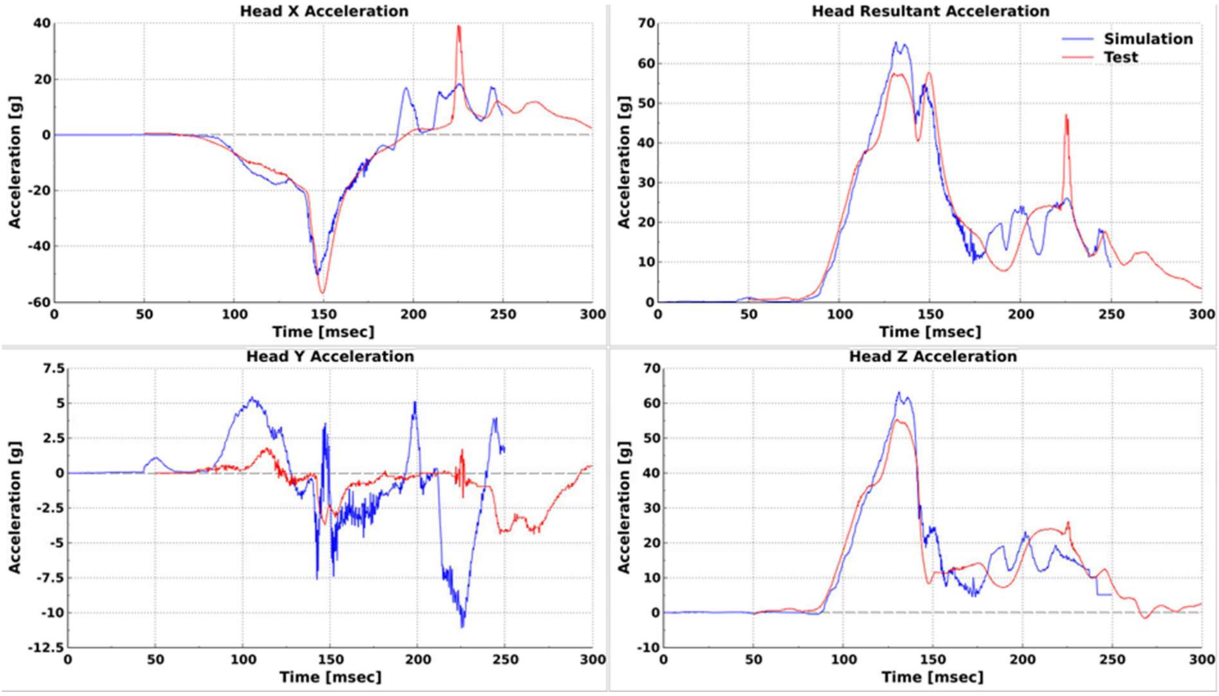

Figure B- 1. Comparison of head acceleration, between physical test (red) and FE simulation (blue)

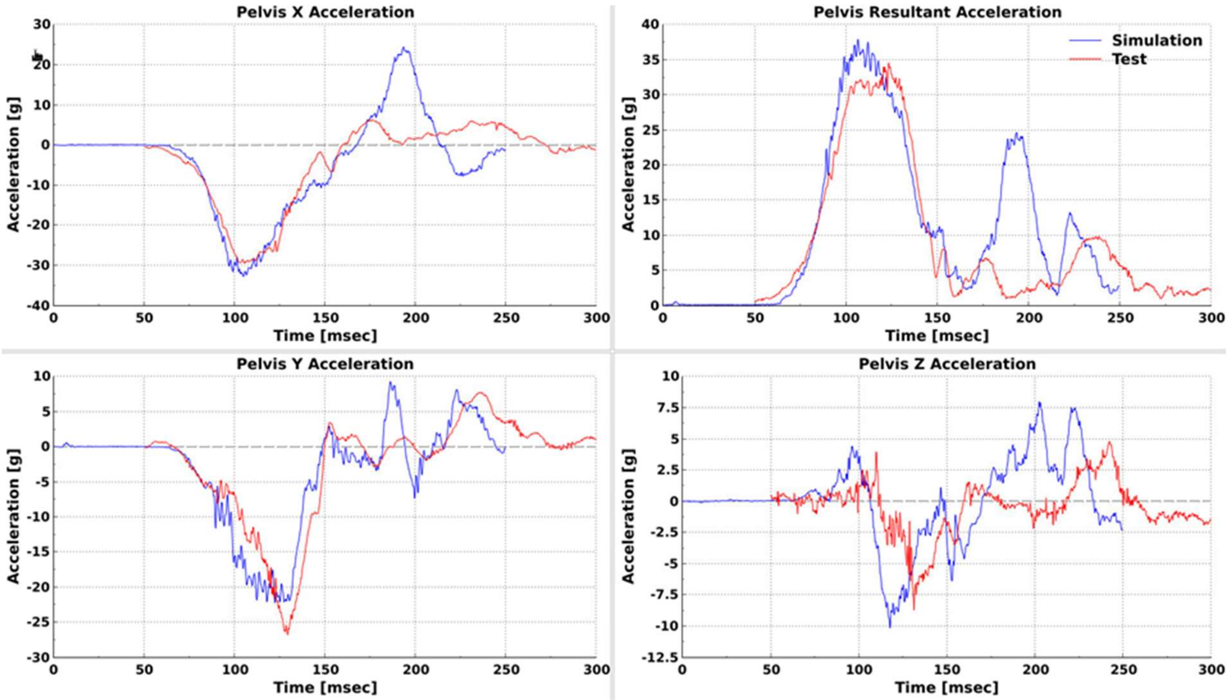

Figure B- 2. Comparison of pelvis acceleration, between physical test (red) and FE simulation (blue)

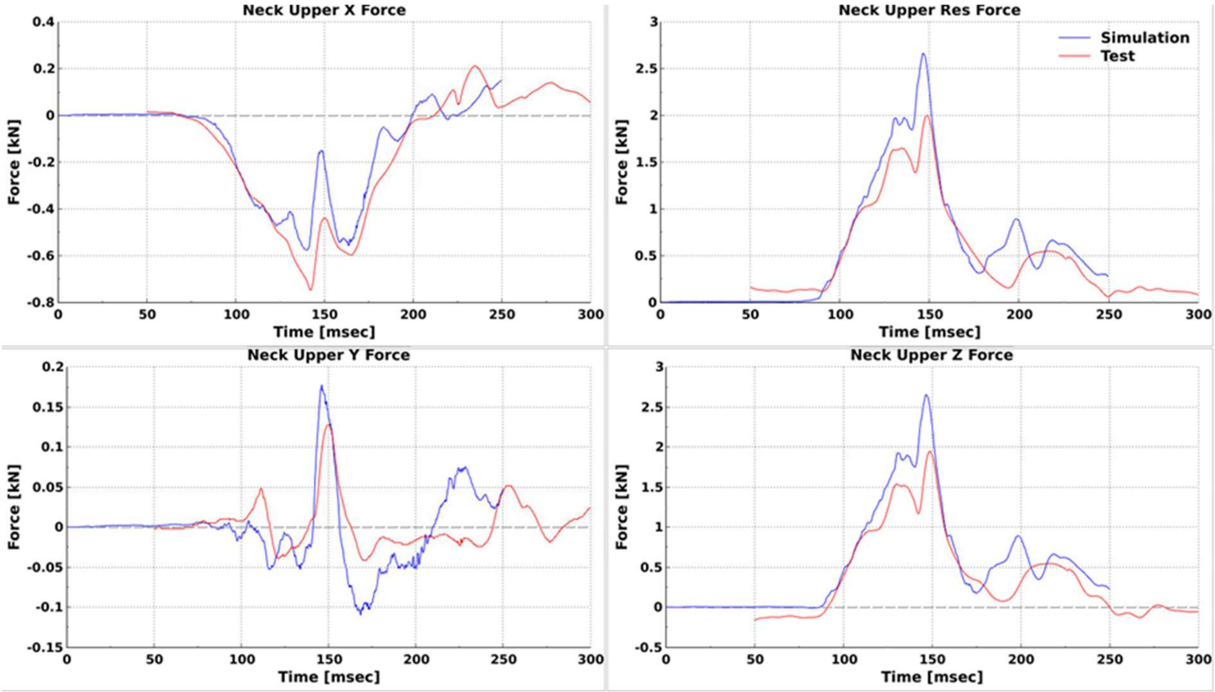

Figure B- 3. Comparison of upper neck force, between physical test (red) and FE simulation (blue)

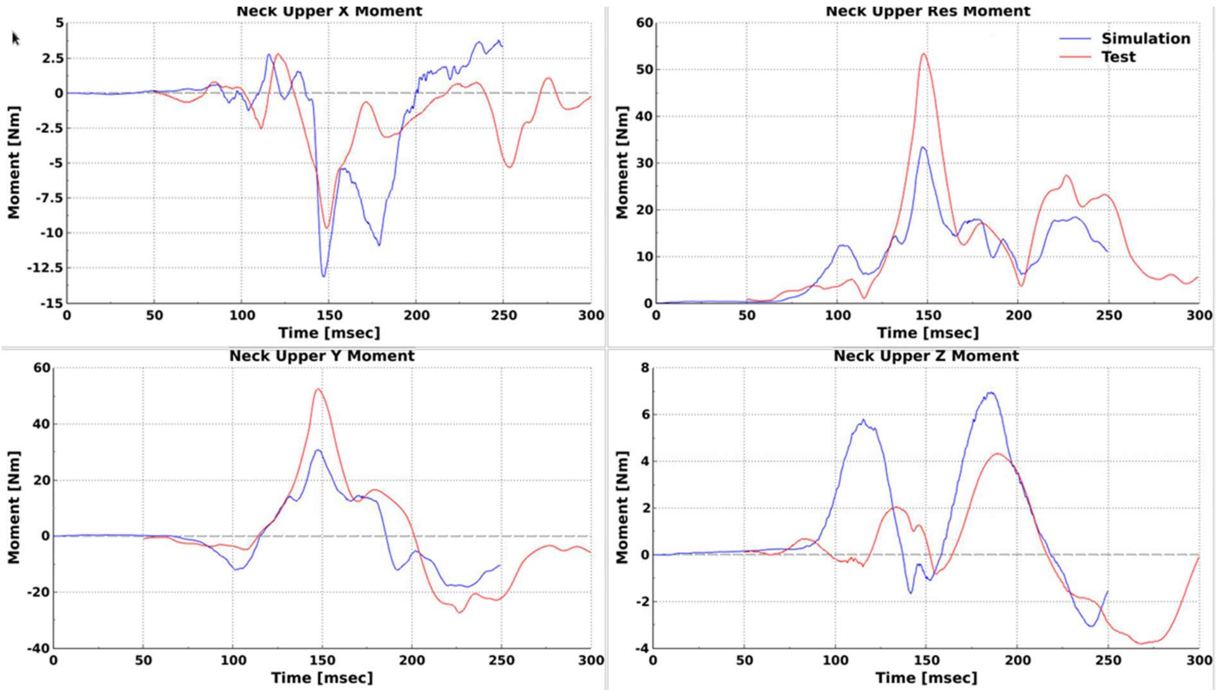

Figure B- 4. Comparison of upper neck moment, between physical test (red) and FE simulation (blue)

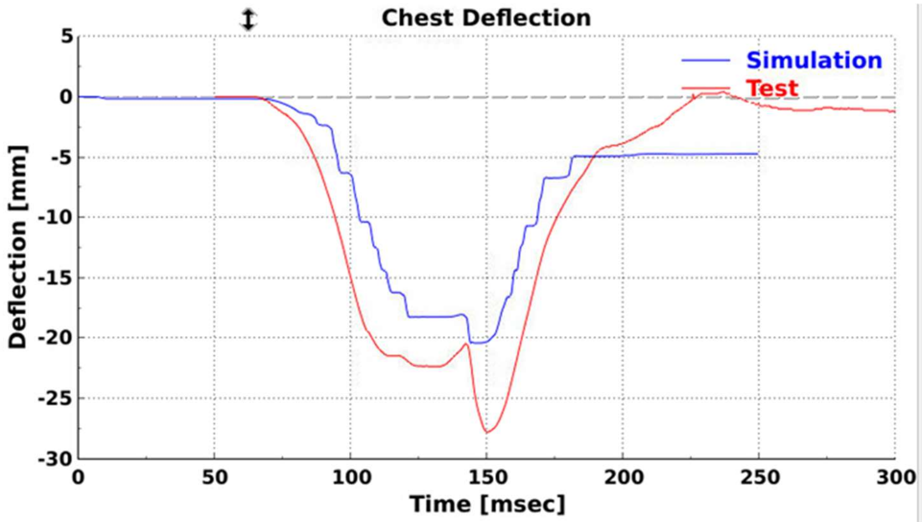

Figure B- 5. Comparison of chest deflection, between physical test (red) and FE simulation (blue)

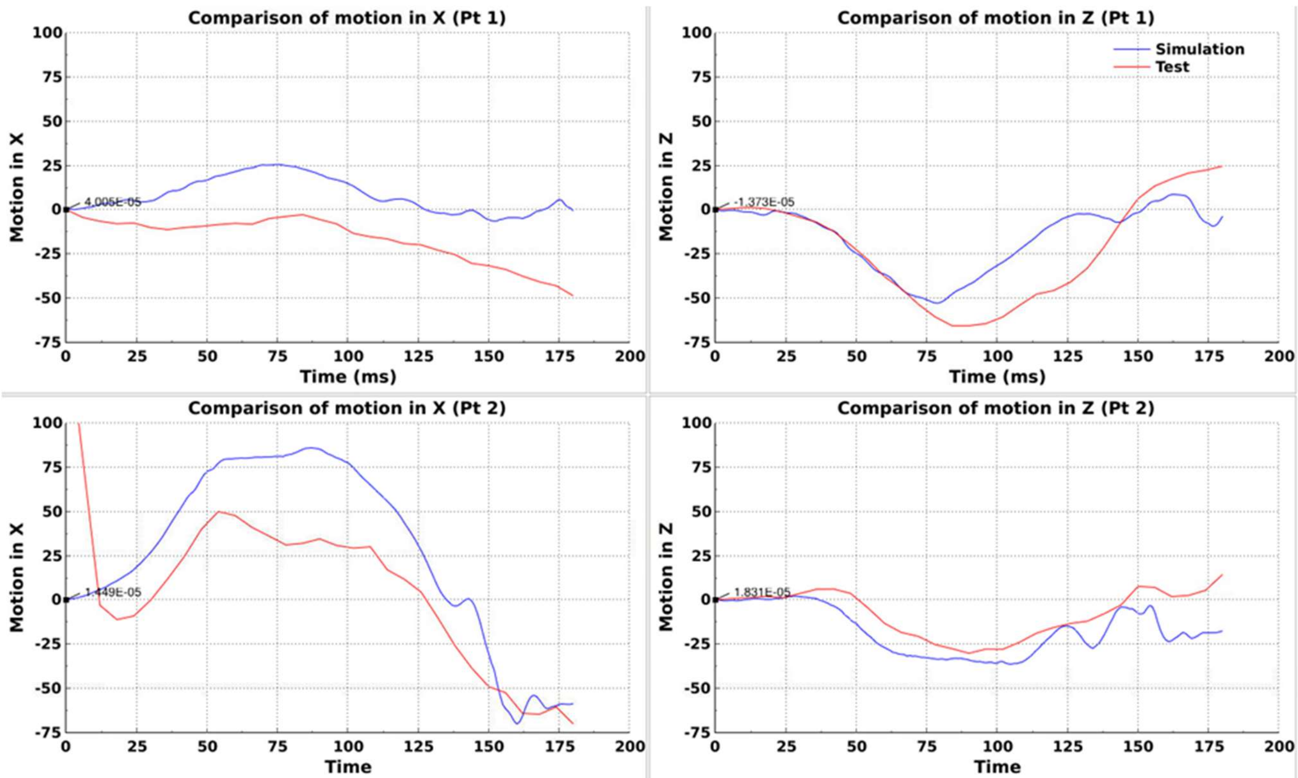

Figure B- 6. Comparison of child seat kinematics, between physical test (red) and FE simulation (blue). Point 1 is located on the front part of the cushion and point 2 on the head rest.

12 Appendix C- Results from the simulation study

In *Table C- 1* the 3ms head accelerations for all simulations can be found.

Table C- 1. Results from the simulation study

Run name	Delta Velocity (dv)	Duration	Head Acceleration 3ms (g)	
			Q6 ATD	PIPER HBM
002	60	94	76.3	68.2
004	50	94	59.9	54.6
005	40	94	43.9	41.3
006	30	94	30.0	27.8
007	60	110	65.1	57.3
008	50	110	51.7	46.7
009	40	110	37.8	36.2
010	30	110	25.8	24.6
011	70	94	93.9	80.8
013	70	110	79.4	68.5
031	80	110	91.3	77.0
037	80	94	111.3	95.7